

Electronic states of 1,3,5-(sym)-triazine. I. Absorption spectra of pure and mixed crystals

E. R. Bernstein and R. E. Smalley

Citation: *The Journal of Chemical Physics* **58**, 2197 (1973); doi: 10.1063/1.1679493

View online: <http://dx.doi.org/10.1063/1.1679493>

View Table of Contents: <http://aip.scitation.org/toc/jcp/58/6>

Published by the *American Institute of Physics*



**COMPLETELY
REDESIGNED!**



**PHYSICS
TODAY**

Physics Today Buyer's Guide
Search with a purpose.

Electronic states of 1,3,5-(*sym*)-triazine. I. Absorption spectra of pure and mixed crystals*

E. R. Bernstein and R. E. Smalley

Department of Chemistry, Princeton University, Princeton, New Jersey 08540

(Received 24 July 1972)

Spectra of pure and isotopic mixed crystals of *sym*-triazine are presented which indicate that the 3455 Å triplet state is $^3E''(n\pi^*)$. These same results confirm previous assignment of the state at 3330 Å as $^1E''(n\pi^*)$. Absorption spectra of *sym*-triazine in *sym*-trioxane chemical mixed single crystals are presented and further corroborate these conclusions. Out-of-plane (parallel) vibrations of *sym*-triazine are considerably affected by crystal fields in both crystal systems. It is demonstrated that assigned state symmetries are not inconsistent with previously obtained experimental results on these states. The nature and type of intermolecular interactions and exciton effects present in the triazine system are briefly discussed. A synthetic route is described which yields substantial quantities of high purity *sym*-triazine, an absolutely essential part of present and forthcoming work on this system.

I. INTRODUCTION

A considerable amount of work has been published within the past few years concerning the lower excited states of *sym*-triazine.¹⁻³ This growing interest is understandable in that *sym*-triazine is apparently an excellent molecule in which to study complexities which arise from orbital degeneracy in an electronic state. Our main interests center about a search to identify and characterize low lying excited states of this molecule through EPR, emission, and absorption studies. In the process of these investigations we have assembled an appreciable body of knowledge concerning the electronic absorption spectra of a variety of isotopically substituted *sym*-triazines. These data have important implications with regard to the nature of a few of these lower excited states. In forthcoming papers⁴ we will discuss observed emission and EPR spectra.

In the process of this work, it was found that commercial sources of *sym*-triazine would not be adequate, in terms of chemical purity and isotopic composition, for our purposes. It was therefore decided to synthesize *sym*-triazine and its deuterated isotopes. Since this synthetic work is believed to be responsible for much of the success of our program, it is reported at some length in Sec. II. It is certain that observation of emission would not have been possible and EPR studies would be useless without high purity isotopic triazines. In Sec. III the results are presented. A detailed discussion of presently reported data and that of other workers is found in Sec. IV.

II. EXPERIMENTAL

The following synthetic scheme is reported completely so that those interested in working on high purity *sym*-triazine may be able to synthesize it. Section II.A is self-contained; it may be passed over by readers concerned only with spectroscopic data and results, without any loss in continuity or logic.

A. Synthesis of *sym*-Triazine

sym-Triazine used in this study was synthesized from HCN and HCl in accord with the initial method of Hinkel and Dunn,⁵ with a few significant variations. The synthesis was carried out entirely in a grease-free high vacuum system. No solvent was used for the initial reaction of HCN and HCl. The product of this reaction was converted to *sym*-triazine through use of Linde Molecular Sieve rather than an organic base such as quinoline which has frequently been used in the past.⁶ The goal in development of this procedure was to eliminate all possible sources of contamination in the final product which might either emit or quench emission in *sym*-triazine crystals. Synthesis of a pure *sym*-triazine sample of mixed isotopic composition is described here, since this synthesis is typical of the many we have done.

The desired isotopic composition for this sample was such that concentration of asymmetric isotopes h_2d_1 and h_1d_2 was as high as possible. This condition obtains when the proton/deuteron ratio is unity. Such a synthesis should produce *sym*-triazine in which the possible isotopes are in the ratio 1:3:3:1 ($h_3:h_2d_1:h_1d_2:d_3$); the mnemonic used for this sample is 1331-*sym*-triazine.

HCN/DCN needed for this synthesis was prepared by the action of H₂O/D₂O on KCN and P₂O₅ in a high vacuum system. The H₂O/D₂O was carefully purified by vacuum distillation, followed by reaction with KMnO₄ and BaO in a sealed tube at 100°C for 7 h, and subsequent vacuum distillations. In order to further insure isotopic as well as chemical purity, all P₂O₅ used was vacuum distilled under controlled temperature conditions (less than 210°C). These steps, as well as all others, were carried out in grease-free vacuum systems operating in the 10⁻⁷ mm Hg range. The only materials in contact with intermediates or product were Pyrex, brass, stainless steel, Kovar, and Teflon. After HCN/DCN was obtained from this reaction, it was dried for several hours *in vacuo* over 2 separate

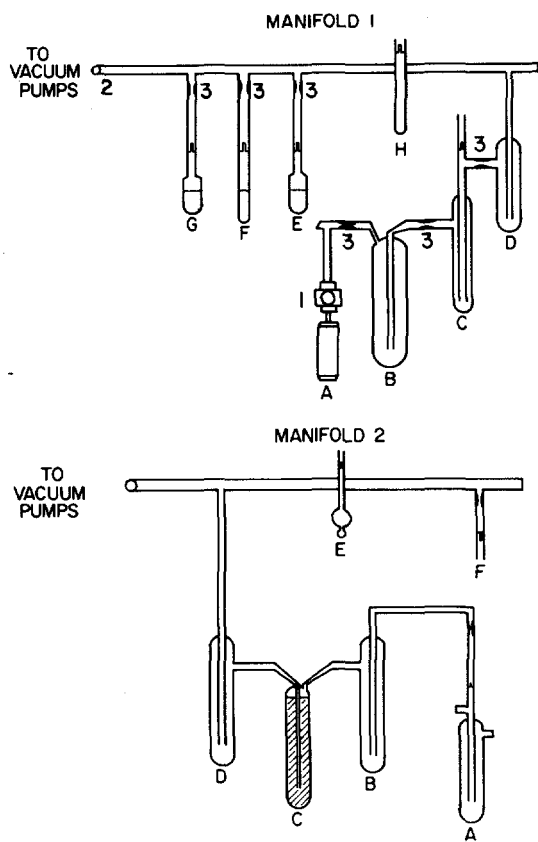


FIG. 1. Manifolds used in the vacuum synthesis of *sym*-triazine. Manifold 1 consists of a 316 stainless steel reaction cylinder (A), bellows valve (1), vacuum traps (B, C, and D); a breakseal tube for removal of excess HCl/DCl at H, and Vessels G, F, and E for introduction of HCl, HCN/DCN, and DCl, respectively. The valve at 2 is a 1 in. brass bellows valve. Vessels are provided with constrictions (3) to allow sealing off under vacuum. Manifold 2 consists of a vessel (A) for introduction of Product II followed by a set of three traps (B, C, D), the center one of which is filled with Linde 5A Molecular Sieve. Vessel E is a quartz optical cell; Vessel F is for storage of the pure *sym*-triazine.

aliquots of P_2O_5 . Vacuum distilled from the P_2O_5 , HCN/DCN was stored at 77°K until required.

Figure 1, Manifold 1 shows the system used in the next step of the synthesis. Vessel A is a 50 cm³ Nupro 316-stainless steel sample cylinder with a Nupro 4BK stainless steel bellows valve connected to the vacuum system with a Kovar-to-Pyrex seal. Vessel F contains 11 ml of the HCN/DCN mixture described above. Vessel E contains 13 ml HCl (Matheson, Electronic Grade) purified by vacuum distillation through several traps cooled to -130°C. Vessel G contains 13 ml of DCl (Merck, Sharp, and Dohme, 99%) purified in a similar manner. HCN/DCN is first distilled into Vessel A; HCl and DCl charges are then simultaneously distilled into the reaction cylinder (held at 77°K) through Traps D, C, and B, each

held at -130°C. The filled reaction cylinder is frozen in liquid nitrogen, degassed, the bellows valve sealed, and the reaction mixture is allowed to warm (from the top down) to -70, 0, and 20°C over a period of a few hours.

The reaction between HCN/DCN and HCl/DCl occurs here at a pressure of 10–20 atm and is quite exothermic; it goes to completion quickly at room temperature, resulting in quantitative conversion of HCN/DCN into the so-called sesquichloride of hydrogen cyanide.^{5,6} This white crystalline highly hygroscopic compound is depicted in Fig. 2(a) and it is referred to as Product I.

After 6 h at room temperature, Vessel A is cooled to 77°K and degassed; normally a small amount of H₂/D₂ is produced. Traps B and C are then cooled -40°C, Trap D is cooled to 77°K, an oil bath is placed around Vessel A, which is gradually heated, and the manifold is continuously pumped through the traps. Excess HCl/DCl, of course, comes off immediately and is trapped at D. Between room temperature and 160°C, roughly 60% of the HCl/DCl which actually reacted to form Product I is recovered in this trap. At 160°C a white material begins to collect in Trap B. This substance [Product II—see Fig. 2(b)] is a mixture of *sym*-triazine and HCl/DCl. Product II is a rather strange, poorly characterized chemical system that appears to have at least two forms. The temperature of Vessel A is slowly increased until Product II ceases to be evolved. The reaction vessel is then glass blown off the system. Trap B is warmed to 20°C, subliming

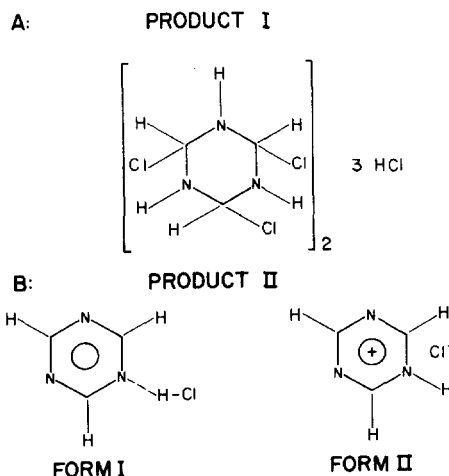


FIG. 2. A: The assumed structure of Product I, the sesquichloride of hydrogen cyanide. B: The assumed structure of the two forms of Product II. This material is believed to be a simple mixture of *sym*-triazine with HCl, dissociated in the gas phase. When condensed, Product II has two forms. Form I is a metastable substance of vapor pressure roughly equal to that of pure *sym*-triazine. Form II is the stable, involatile salt. This salt decomposes at 160°C into *sym*-triazine+HCl along with small amounts of H₂, HCN, and other uncharacterized products.

Product II into C where it is trapped at -40°C ; this trap is then immersed in liquid nitrogen and sealed off on both sides under vacuum. Product II must be stored under liquid nitrogen until needed for subsequent steps in the synthesis. The over-all yield of Product II from Product I is normally 90%–95%.

Figure 1, Manifold 2, shows the vacuum system used to remove HCl/DCl from Product II. This step yields pure *sym*-triazine. Vessel A contains Product II from Manifold 1. Vessel C is a trap which contains ~ 0.6 liter of 5A Molecular Sieve ($\frac{1}{8}$ in. pellets). The adsorbent had been previously regenerated and degassed by pumping to 1×10^{-6} mm Hg in a vacuum system for 2 days at 300°C . Workup of Product II is straightforward. Vessel D is cooled to -90°C and Vessel A is brought to room temperature while the system is pumped. Product II sublimates easily through Trap C and *sym*-triazine immediately collects in Vessel D. After all Product II has passed into the adsorbent bed, Vessel A is sealed off and *sym*-triazine which has been collected in Vessel D is sublimed up to Quartz Cell E for immediate spectroscopic investigation, and to Vessel F for storage.

Yield of *sym*-triazine is only about 60% over-all for this synthesis. Reduced yield is due almost entirely to *sym*-triazine adsorbed on the surface of Molecular Sieve in Vessel C. Most of this can be recovered by heating the adsorbent to 200°C . The HCl/DCl is irreversibly adsorbed, however. We have chosen not to recover this adsorbed *sym*-triazine since we are at this stage more concerned with purity than yield.

B. Purification of *sym*-Triazine

Many methods have been tried, with varying degrees of success, to purify *sym*-triazine. Use of Molecular Sieve as described above appears to be best. All *sym*-triazine samples used in work reported herein were purified in this fashion before their spectra were recorded.

C. Purification of Trioxane

Trioxane is one of the few molecular organic crystals which is uniaxial at low temperature⁷ and transparent in the ultraviolet to 2100 \AA . Because trioxane polymerizes to polyoxymethylene in the presence of trace amounts of formaldehyde,⁸ it has not been often used as a host for chemical mixed crystal systems.

The problem of polyoxymethylene formation may be temporarily alleviated by fusing trioxane in a sealed, evacuated breakseal tube with ~ 1 g of LiAlH_4 .⁹ The mixture is kept at roughly 90°C until trioxane is needed as a mixed crystal host. It is then distilled from the breakseal tube and for a while this trioxane will behave in a vacuum system like any standard material. Thus treated, large (10 cm) single crystals of glasslike quality may be melt or vapor grown. Normally there is sufficient time to load trioxane into a Bridgeman

tube, seal it off the vacuum system, and grow a single crystal from the melt before any polyoxymethylene forms. Depolymerization of trioxane is catalyzed by acidic compounds,⁸ thus presence of *sym*-triazine in these mixed crystals is undoubtedly a stabilizing influence.

It has been possible to prepare high optical quality mixed crystals of 2% *sym*-triazine in trioxane. Mixed crystals of glasslike appearance have been grown up to 10 cm in length, over a period of almost a week, and yet no observable polyoxymethylene was formed.

D. Spectroscopic Apparatus and Techniques

All spectra were taken on a McPherson 2 m, $f/17$, Czerny–Turner spectrograph. Typically, this instrument was used in second order at a dispersion of $1.8 \text{ \AA}/\text{mm}$. Most spectra were recorded on Kodak 103 a-O plates, although a few experiments required the higher sensitivity attainable with a photon counting apparatus recently assembled in this laboratory.⁴

Crystals from which spectra were obtained were prepared by both vapor and melt growth techniques. Most synthesis-prepared samples (Sec. II.A) were grown directly into quartz optical cells and were, therefore, never exposed to air during the entire course of these experiments. No attempt was made to orient such crystals; observed intensity ratios are therefore somewhat modulated by uncertainty as to the angle between crystal optic axes and light propagation direction. In thin crystals (≤ 0.5 mm) many crystal orientations were present in the cross section perpendicular to the direction of light propagation. Longer crystals were, however, quite definitely single; in these cases, optic axis orientation is indicated to the extent that it is known.

All frequency measurements are vacuum corrected and are accurate to within 0.5 cm^{-1} for sharp lines.

Our results concur with those of earlier workers^{1,2} in that the phase transition to a monoclinic, optically biaxial, triply twinned form at $T \leq -60^{\circ}\text{C}$ ¹⁰ does not affect optical quality of *sym*-triazine crystals. It is possible to cool repeatedly single crystals up to 3.3 cm in length to 4.2°K without formation of any cracks. Trioxane crystals behave similarly.

III. RESULTS

A. Spectra of h_3 - and d_3 -*sym*-Triazine Crystals

Figure 3 presents the absorption spectrum of 1 and 0.1 mm crystals of h_3 -*sym*-triazine, as synthesized by techniques outlined in Sec. II.A. These spectra are identical to those of equivalent crystals prepared from various commercial sources of *sym*-triazine. For convenience in ensuing discussions, different regions of this spectrum will be labeled as indicated in the figure. Figure 4 presents the absorption spectrum of a 2.5 mm crystal of the same h_3 -*sym*-triazine at longer wave-

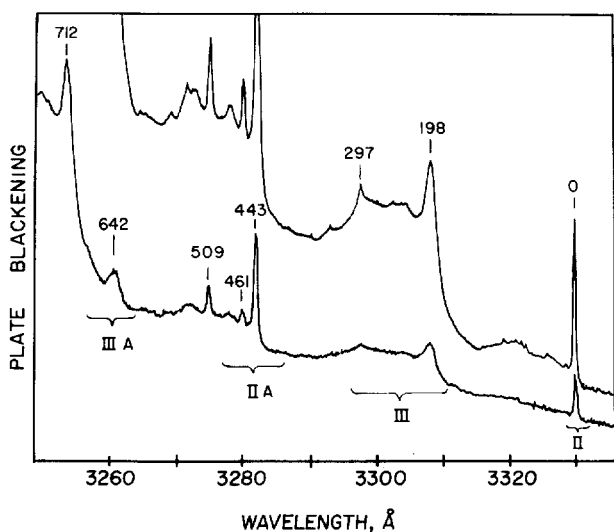


FIG. 3. Absorption spectrum at 4.2°K of h_3 -*sym*-triazine crystals ~ 0.1 and 1.0 mm thick. The $C_3N_3H_3$ for these experiments was synthesized as outlined in Sec. II.A. Distance in cm^{-1} from the origin (Region II, $30\,014.0 \pm 0.2\,cm^{-1}$) is indicated above each absorption feature. Optic axis orientation was not known for these samples. Regions II, III, IIA, and IIIA, as discussed in the text, are indicated under the spectrum.

length. Absorption at 3455 Å (Region I) is quite sharp and may easily be seen in crystals of 1.5 mm thickness. Figure 5 presents absorption in this same region due to a 33.0 mm crystal of h_3 -*sym*-triazine (from K & K Laboratories). The sudden and dramatic broadening of features immediately blue of the sharp

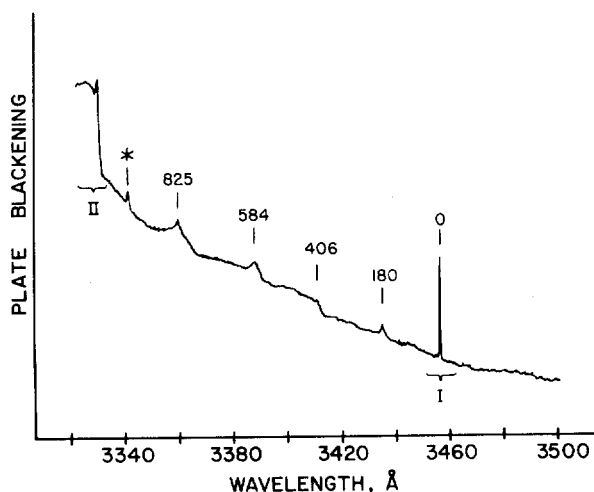


FIG. 4. Long wavelength (Region I to Region II) absorption spectrum at 4.2°K of a 2.5 mm crystal of h_3 -*sym*-triazine as synthesized by the method of Sec. II.A. The absorption marked with an asterisk is due to the ${}^1B_{3u}$ (0-0) transition of pyrazine which was accidentally allowed to contaminate this particular sample. This transition appears here at $29\,917.0 (\pm 0.5)\,cm^{-1}$. The distance in cm^{-1} from the origin (Region I, $28\,935.1 \pm 0.2\,cm^{-1}$) is marked above the major absorption features.

origin (Region I) is much like that found in 2,6-dimethyl pyrazine¹¹ and may well be due to interaction with a second, probably unobserved, electronic state. Fine structure about the main absorption in Region I was further explored using a photon counting apparatus. A typical output histogram presentation is given in Fig. 6(a). The weak absorption features to high and low energy of the main peak at $3455.02\,Å$ are believed due to ${}^{13}C^{12}C_2N_3H_3$ and ${}^{15}NC_3^{14}N_2H_3$ in natural abundance. Reasonably sharp structure between 20 and $120\,cm^{-1}$ from Region I is quite similar to that found in Region II and is very possibly attributable to phonon

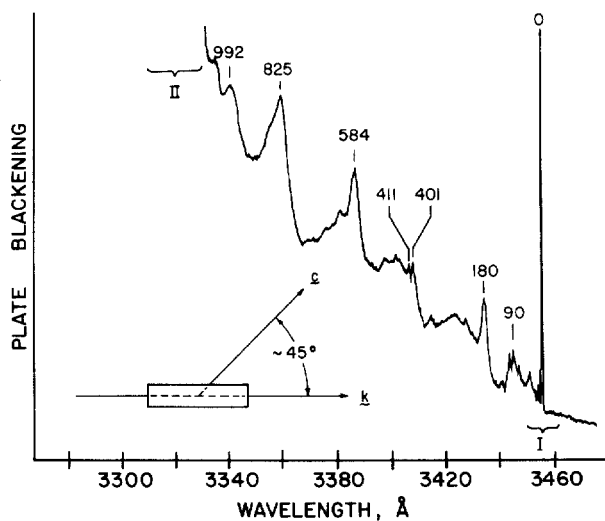


FIG. 5. Absorption spectrum of a 3.3 cm single crystal of h_3 -*sym*-triazine at 4.2°K. This sample was melt grown from commercially obtained material (K & K Laboratories, Inc.) which had been purified by passage over Molecular Sieve. The relative orientation of the optic axis c with respect to the direction of light propagation k is indicated in the inset of this figure. We have observed no absorption lines in this sample at wavelengths greater than 3456 Å. Numbers indicated over various features are distances in cm^{-1} of the specific feature from the origin at $28\,935.1 \pm 0.2\,cm^{-1}$. Regions I and II, discussed in the text, are indicated under the spectrum.

addition to the origin at $3455.02\,Å$. No absorption whatsoever in *sym*-triazine has been observed at higher wavelength than Region I. Virtually identical structure is found associated with Region II spectra and can be attributed to similar causes. Figure 6(b) shows a microdensitometer tracing of ${}^{15}NC_3N_2D_3$ and ${}^{13}CC_2N_3D_3$ features about the $C_3N_3D_3$ Region II absorption.

Figures 7 and 8 show the absorption in Regions I, II, and III for a crystal of d_3 -*sym*-triazine as synthesized by techniques described previously. Sharp absorption at $3340.68\,Å$ is due to the ${}^1B_{3u}$ origin of pyrazine which was inadvertently allowed to contaminate this particular crystal. The two features at 3322.79 and $3320.03\,Å$ in Fig. 8 are due to d_2h_1 -*sym*-triazine which was made in the original synthesis to an extent

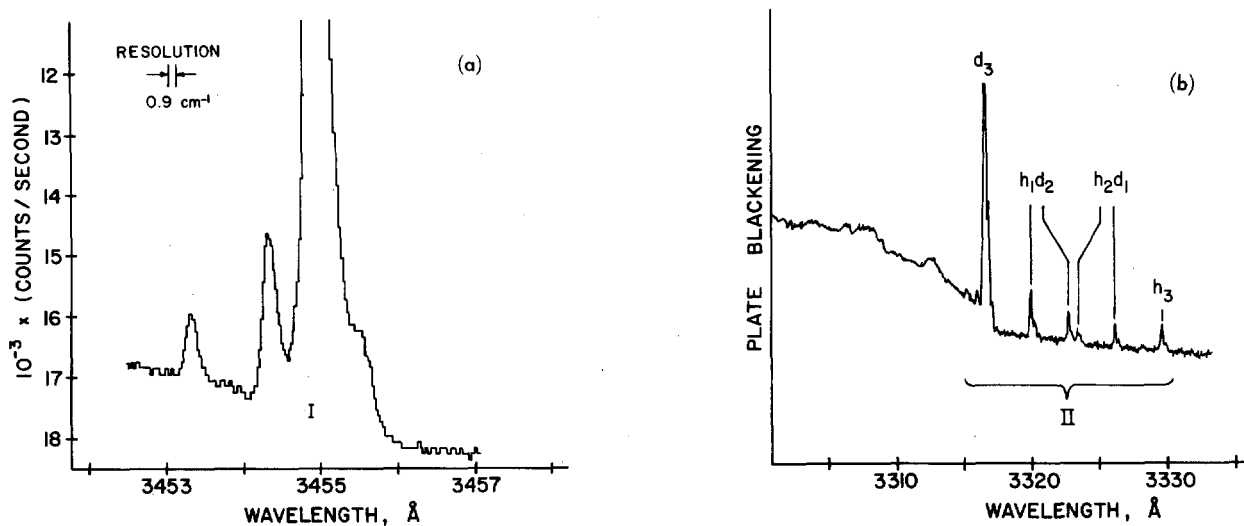


FIG. 6. (a) Expanded trace of the absorption spectrum at 3455 Å of the 3.3 cm h_3 -*sym*-triazine crystal (same as in Fig. 5). Peak absorption of the main line occurred at ~ 1500 cps. The three small absorption features surrounding the main line are believed to be due to $^{13}\text{C}^{12}\text{C}_2\text{N}_3\text{H}_3$ and $^{15}\text{N}\text{C}_3^{14}\text{N}_2\text{H}_3$ in natural abundance. These features appear at $28\,930.7 \pm 0.2$, $28\,940.5 \pm 0.2$, and $28\,948.7 \pm 0.2$ cm^{-1} . Distances from the main absorption at $28\,935.1 \pm 0.2$ cm^{-1} are therefore -4.4 , $+5.4$, $+13.6$ cm^{-1} . (b) Region II absorption at 4.2°K of a 1.5 mm d_3 -*sym*-triazine sample which contained $\sim 4\%$ 1331-triazine and $\sim 1\%$ h_3 -*sym*-triazine. This is a different crystal grown from the same material used in the experiment shown in Fig. 9. The lines shown by this crystal in Region II are the sharpest we have ever observed. Due to this increased sharpness, $^{13}\text{C}/^{15}\text{N}$ absorptions in Region II are now clearly revealed. The three lines about the d_3 Region II absorption (30 142.9 cm^{-1}) are separated from this absorption by -2.8 , $+4.8$, and $+12.2$ cm^{-1} , respectively. Note that satellite lines are observed to the red of all absorptions in this crystal, including those of all isotopic guest molecules. It is believed that the strength of the absorption red of the d_3 (host) absorption is at least in part due to a guest-host perturbed feature in this highly doped crystal. See Secs. IV.G and IV.I for a more complete discussion.

of about 0.75%. To be particularly noted is that *Region II* absorption for d_2h_1 -*sym*-triazine is split into two lines, of nearly equal intensity, separated by 25 cm^{-1} . Figure 9 represents absorption in this region due to a d_3 -*sym*-triazine crystal which had been doped with

$\sim 1\%$ h_3 -*sym*-triazine and $\sim 4\%$ 1331-*sym*-triazine. Here Region II absorption of all hydrogen-deuterium isotopic species of *sym*-triazine is clearly resolved. Region II absorption is split by 25 cm^{-1} for both C_{2v} isotopes.

B. Spectra of 1331-*sym*-Triazine Crystals

The 1331-*sym*-triazine samples were synthesized in order to study spectra of the C_{2v} isotopes more completely. Figure 10 shows absorptions in Regions II, III, IIA of a 0.5 mm crystal of 1331-*sym*-triazine. Absorption in Region II confirms earlier observations in d_3 -*sym*-triazine host crystals. Relative integrated intensities of features due to the various isotopes is very roughly in the ratio of 1:3:3:1, thereby confirming that there are three equivalent hydrogen positions on the molecule responsible for this absorption. More will be said about this intensity pattern in Secs. IV.A and IV.I.

Absorption in Region III due to C_{2v} isotopic species does not appear to be split. Absorptions at higher energy than Region III are too broad and/or complex for simple interpretation. Note that all absorption widths in the 1331 crystal have markedly increased.

Figure 11 shows the absorption in Region I of a 5 mm crystal of 1331-*sym*-triazine. Clearly, the same phenomenon responsible for the splitting pattern in Region II has also produced a splitting of h_2d_1 -*sym*-

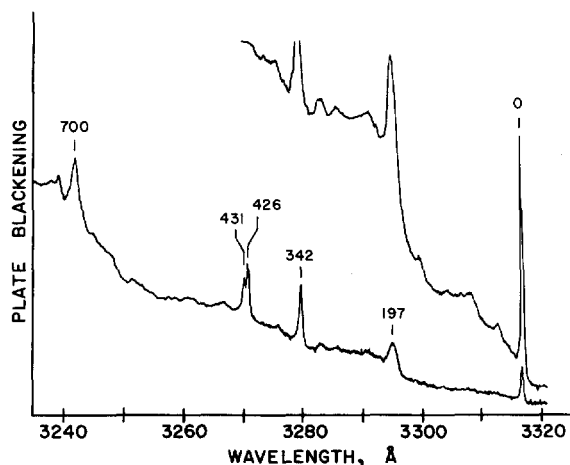


FIG. 7. Absorption spectrum at 4.2°K of d_3 -*sym*-triazine crystals ~ 0.1 and 1.0 mm thick. The $\text{C}_2\text{N}_3\text{D}_3$ for these experiments was synthesized as outlined in Sec. II.A. Distance in cm^{-1} from the origin (Region II, 30 142.9 ± 0.2 cm^{-1}) is indicated above each absorption feature. Optic axis orientation was not known for these samples.

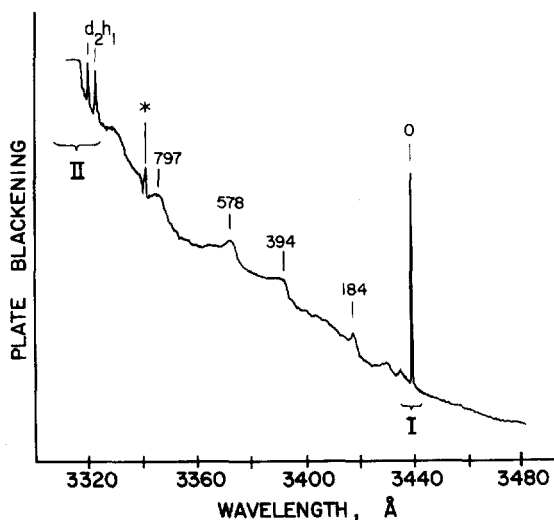


FIG. 8. Long wavelength (Region I to Region II) absorption spectrum at 4.2°K of a 3 mm crystal of d_3 -*sym*-triazine as synthesized by the method of Sec. II.A. The absorption marked with an asterisk is due to the ${}^1B_{3u}$ (0-0) transition of pyrazine which was accidentally allowed to contaminate this particular sample. This transition appears here at $29\,925.4 \pm 0.5$ cm^{-1} . Distance in cm^{-1} from the origin (Region I, $29\,077.6 \pm 0.2$ cm^{-1}) is marked above the major absorption features. The absorption due to the $\sim 0.75\%$ $\text{C}_2\text{N}_3\text{D}_2\text{H}$ impurity in this sample may be clearly seen in Region II. This absorption is split into two lines appearing at $30\,086.5 \pm 0.2$ cm^{-1} and $30\,111.5 \pm 0.2$ cm^{-1} . Optic axis orientation was unknown for this sample.

triazine and h_1d_2 -*sym*-triazine absorptions in Region I. In neat crystals of h_3 -*sym*-triazine, absorption linewidth of Region I is ~ 0.9 cm^{-1} as compared to usually 3 cm^{-1} for Region II lines [see, however, Sec. IV.I and Fig. 6(b)]; in 1331 crystals h_3 -*sym*-triazine absorption linewidth in both regions is of the order of 5-7 cm^{-1} . A further point to mention concerning this sample, and the *sym*-triazine system in general, is that, to within the 1331 crystal linewidths, both pure and mixed crystal $h_3(d_3)$ -*sym*-triazine absorptions coincide in both Regions I and II (see Fig. 12). This experimental finding has important ramifications for intermolecular interactions in the *sym*-triazine system and will be discussed in more detail later (Secs. IV.E and IV.H).

C. Trioxane Chemical Mixed Crystal Spectra

The absorption due to approximately 2% h_3 -*sym*-triazine in 5 and 1 cm single crystals of trioxane is given in Fig. 13. Region II absorption in pure *sym*-triazine crystals has been blue shifted 518.6 cm^{-1} , but its intensity and linewidth have been altered only slightly. Sharp features in Region IIA have moved closer to Region II and broadened somewhat. In general, the h_3 -*sym*-triazine spectrum has not altered much except for Region III in which profound changes have occurred as a result of changing crystalline environ-

ment. It is not at all clear how one can make a detailed correlation of features between trioxane and *sym*-triazine crystal spectra in this region. Figure 14 presents the resultant spectra in Regions II, III, and IIA for 1/2% d_3 -*sym*-triazine in 2.8 and 6.0 cm crystals of trioxane. Again the out-of-plane vibrations, particularly in Region III, are most perturbed by the trioxane crystal field.

A mixed crystal of 1331-*sym*-triazine was prepared in order to determine the effect of the trioxane crystal site on Region II absorption of C_{2v} isotopic species. Figure 15 compares results of this experiment with the splitting pattern observed earlier in pure 1331-*sym*-triazine crystals. It is not possible to give a detailed interpretation of 1331-*sym*-triazine/trioxane sample absorption in Region II due to overlap with Region III and the high probability of pair spectra in such a heavily doped sample. The sharp absorption 12.8 cm^{-1} to the red of the main Region II line in a 2% h_3 -*sym*-triazine/trioxane crystal (Fig. 13) may well be attributable to "resonance pair" spectra.

At the present time trioxane is the only chemical mixed crystal host known for *sym*-triazine. Owing to the forbidden nature of the lowest excited states of *sym*-triazine, extremely long (about 2-5 cm) mixed crystals of high concentrations are needed. Hosts must be, therefore, extraordinarily pure and capable of incorporating large amounts of *sym*-triazine into

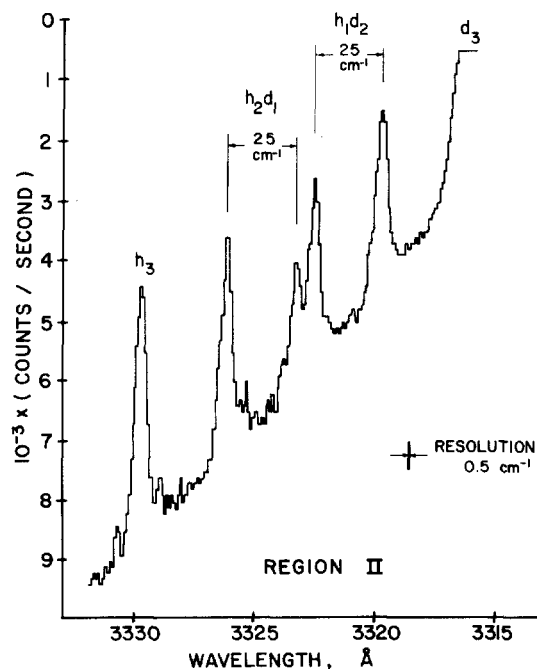


FIG. 9. Region II absorption spectra taken at 4.2°K using a photon counting apparatus for detection. The sample is a 2 mm single crystal of d_3 -*sym*-triazine doped with approximately 4% 1331-*sym*-triazine and 1% h_3 -*sym*-triazine. The optic axis orientation is unknown for this experiment. Exact line positions are listed in Table I.

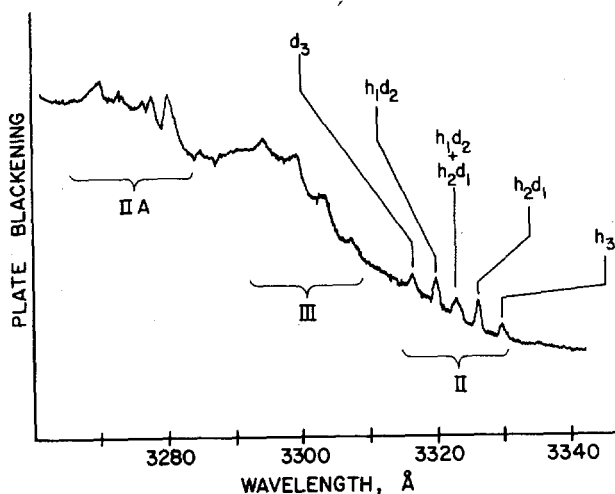


FIG. 10. Absorption spectrum at 4.2°K of a 0.5 mm crystal of 1331-*sym*-triazine. Optic axis orientation is not known. Region III absorptions appear at 30 217, 30 259, 30 295, and 30 338 cm^{-1} for the h_3 , h_2d_1 , h_1d_2 , and d_3 species, respectively. Exact energies for the Region II transitions are listed in Table I.

their crystal lattices. Benzene, durene, borazine, cyanuric chloride, and methyl cyclohexane have been tried as host crystals with no success. *sym*-Triazine appears to have great difficulty in forming mixed crystals with hydrocarbon hosts.

Table I contains all numerical data for Regions I and II discussed above and in the following section.

IV. DISCUSSION

These spectral results clearly show that absorption in Regions I and II are due to electronic transitions of the same molecule. Splitting patterns for various isotopic species are much too similar to be ascribed to

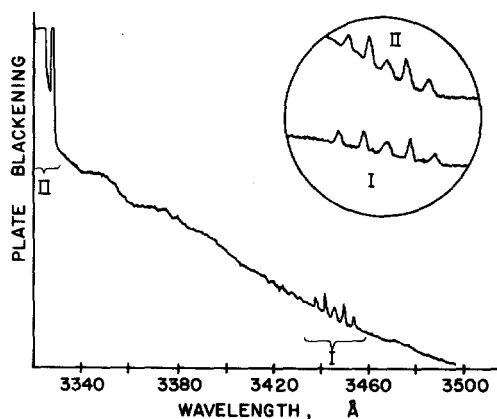


FIG. 11. Absorption spectrum at 4.2°K of a 5.0 mm crystal of 1331-*sym*-triazine. Optic axis orientation is not known. Exact energies for the Region I transition of the various isotopes are listed in Table I. The insert compares the absorption of this 5 mm sample in Region I with the Region II absorption of a 0.5 mm 1331-*sym*-triazine crystal.

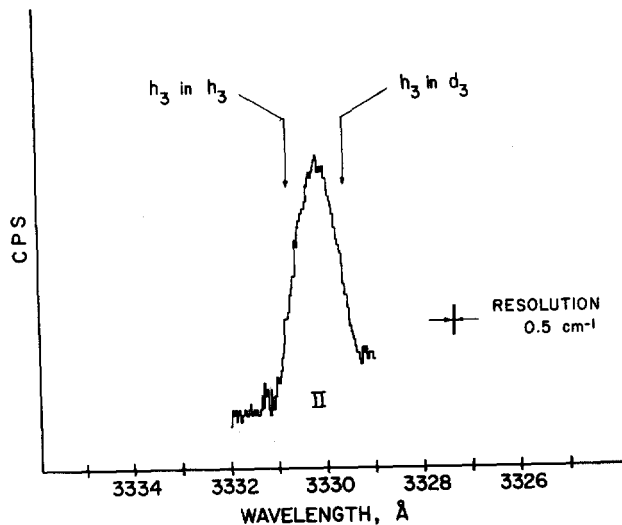


FIG. 12. A high resolution phototube trace of the Region II absorption of $\text{C}_2\text{N}_2\text{H}_2$ in a 1 mm 1331-*sym*-triazine crystal at 4.2°K. The position of this absorption in $\text{C}_2\text{N}_2\text{H}_2$ and $\text{C}_2\text{N}_2\text{D}_2$ host crystals is shown to illustrate the relation of these positions to the linewidth of the absorption in a 1331 crystal.

different molecules. Relative intensity and number of lines for 1331 samples indicate that the molecule has three equivalent hydrogen positions. The Zeeman effect results¹ on Region II clearly show that the transition responsible for this absorption involves an orbitally degenerate (upper) electronic state; thus, the molecule has at least a threefold axis of symmetry. Absorptions in both Region I and Region II are

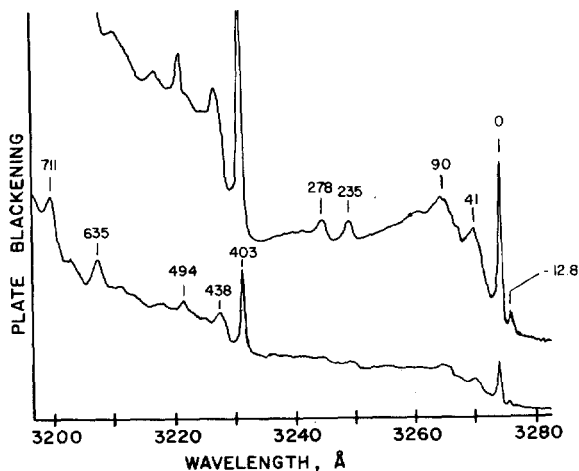


FIG. 13. Absorption spectra at 4.2°K of 2% h_3 -*sym*-triazine in *sym*-trioxane mixed crystals 5.0 and 1.0 cm in length. Both of these samples were oriented such that the angle between the threefold crystal axis and the direction of light propagation was $\sim 30^\circ$. The distance in cm^{-1} from the origin (Region II, $30\,532.6 \pm 0.2\, \text{cm}^{-1}$) is marked above the major absorption features. The weak line $12.8\, \text{cm}^{-1}$ red of the origin is probably due to a $\text{C}_2\text{N}_2\text{H}_2$ pair. In this regard compare with Fig. 14.

TABLE I. Measured positions for the origins of the transitions ${}^3E'' \leftarrow {}^1A_1'$ (Region I) and ${}^1E'' \leftarrow {}^1A_1'$ (Region II) of the various isotopes of *sym*-triazine in pure and mixed crystals.

Guest	λ (air), Å	$\bar{\nu}$ (vacuum), cm^{-1}	Guest	λ (air), Å	$\bar{\nu}$ (vacuum), cm^{-1}
Region I			Region II (continued)		
Host = <i>h</i> ₈ - <i>sym</i> -triazine			Host = 1331- <i>sym</i> -triazine		
C ₃ N ₃ H ₃	3455.02±0.02	28 935.1±0.2	C ₃ N ₃ H ₃	3330.21±0.05	30 019.5±0.5
	3455.54	28 930.7	C ₃ N ₃ H ₂ D ₁	3326.75	30 050.7
¹³ C ¹² C ₂ N ₃ H ₃	3454.37	28 940.5	C ₃ N ₃ H ₁ D ₂	3323.71	30 078.2
¹⁵ NC ₃ ¹⁴ N ₂ H ₃	3453.40	28 948.7		3320.56	30 106.7
			C ₃ N ₃ D ₃	3317.01	30 139.0
Host = 1331- <i>sym</i> -triazine			Host = <i>d</i> ₃ - <i>sym</i> -triazine		
C ₃ N ₃ H ₃	3454.44±0.05	28 940.0±0.5	C ₃ N ₃ H ₃	3329.70±0.02	30 024.1±0.2
	3450.28	28 974.9	C ₃ N ₃ H ₂ D ₁	3326.22	30 055.5
C ₃ N ₃ H ₂ D ₁	3446.53	29 006.4		3323.46	30 080.5
C ₃ N ₃ H ₁ D ₂	3442.63	29 039.2	C ₃ N ₃ H ₁ D ₂	3322.79	30 086.5
				3320.03	30 111.5
C ₃ N ₃ D ₃	3438.41	29 074.9	C ₃ N ₃ D ₃	3316.58	30 142.9
				3316.88	30 140.1
Host = <i>d</i> ₃ - <i>sym</i> -triazine				3316.05	30 147.7
C ₃ N ₃ D ₃	3438.09±0.02	29 077.6±0.2	¹³ C ¹² C ₂ N ₃ D ₃	3315.24	30 155.1
			¹⁵ NC ₃ ¹⁴ N ₂ D ₃		
Region II			Host = <i>sym</i> -trioxane		
Host = <i>h</i> ₃ - <i>sym</i> -triazine			C ₃ N ₃ H ₃	3275.62°±0.02	30 519.8°±0.2
C ₃ H ₃ N ₃	3330.82±0.02	30 014.0±0.2		3274.24	30 532.6
			C ₃ N ₃ H ₂ D ₁	3272.14°	30 552.2°
¹³ C ¹² C ₂ N ₃ H ₃	3330.30	30 018.7		3270.94	30 563.4
¹⁵ NC ₃ ¹⁴ N ₂ H ₃	3329.47 ^a	30 026.2 ^a		3268.40	30 587.2
			C ₃ N ₃ H ₁ D ₂	3265.0±2 ^d	30 620.0±20 ^d
C ₃ H ₃ D ₃	3317.37±0.05 ^b	30 135.7±0.5 ^b	C ₃ N ₃ D ₃	3263.02°±0.02	30 637.6°±0.2
				3261.67	30 650.3

^a The other expected ¹³C/¹⁵N features are not seen in any of the C₃N₃H₃ samples we have examined. Such features probably have been obscured by the ~3 cm⁻¹ linewidth of the ¹²C₂¹⁴N₃H₃ absorption.

^b This result is for a sample of C₃N₃H₃ which contained ~10% C₃N₃D₃. The Region II absorption lines for both of these species

identical in *h*₃-*sym*-triazine samples made by two entirely different synthetic routes,¹² and both absorptions are unaffected by any sample purification or manipulation technique. These facts constitute a proof that the observed absorptions must be due to *sym*-triazine.

A. C_{2v} Isotopes—Region I and Region II Spectra

Doubling of observed features in Regions I and II for *d*₂*h*₁- and *d*₁*h*₂-*sym*-triazine isotopic species (see Table I and Figs. 8–11, 15) under conditions for which *d*₃- and *h*₃-*sym*-triazine (Table I and Figs. 6–8) remain

in this sample were asymmetrically broadened to higher energies. After taking this effect into account, we estimate the position of this line at infinite dilution to be 30 133±0.5 cm⁻¹.

^c These absorptions are probably due to resonance pairs.

^d Absorption in this region is obscured by Region III absorption and probable resonance pair features.

single, can be explained only in the following three ways:

1. The splitting may be due to a difference in gas-to-crystal shift Δ for two inequivalent orientations of C_{2v} molecules in a site of effective symmetry lower than C₃.

2. The splitting may be due to removal of a vibrational degeneracy in these isotopes. Regions I and II absorption features then correspond to electronic transitions wherein an *e'* or *e''* vibrational mode is excited in the upper state.

3. The splitting may be due to removal of an elec-

tronic (or vibronic) degeneracy in these isotopes. This possibility will be termed the *zero point effect* in the sections that follow.

Results from trioxane mixed crystals confirm conclusions reached by Fischer and Small² recently that the lowest observed gas phase electronic transition corresponds to *sym*-triazine Region II crystal absorption. Their hot band assignments rule out the possibility that Region II absorption is a false origin, rendering explanation 2 (above) highly unlikely.

Of the remaining two explanations, only possibility 1 is a crystal effect. The definitive experiment would be, therefore, gas phase absorption of Regions I and II. Unfortunately, Region II absorption in the vapor is obscured by hot bands²; observation of Region I absorption, while possible in principle, would require prohibitively long path lengths and would probably be obscured by Region II hot band structure.² In lieu of such an experiment, the following plausibility arguments can be assembled to distinguish between explanations 1 and 3 above:

(a) All evidence collected thus far for *sym*-triazine indicates that deviation from threefold symmetry in the crystal is extremely small. Orientational effects^{13a} are therefore expected to be much smaller than those found in other, less symmetrical crystals such as benzene.¹³ A 25 to 30 cm^{-1} orientational effect for hydrogen-deuterium substitution would easily be the largest such effect yet observed in an organic molecular crystal. An orientational effect of this magnitude is certainly not expected in *sym*-triazine crystals.

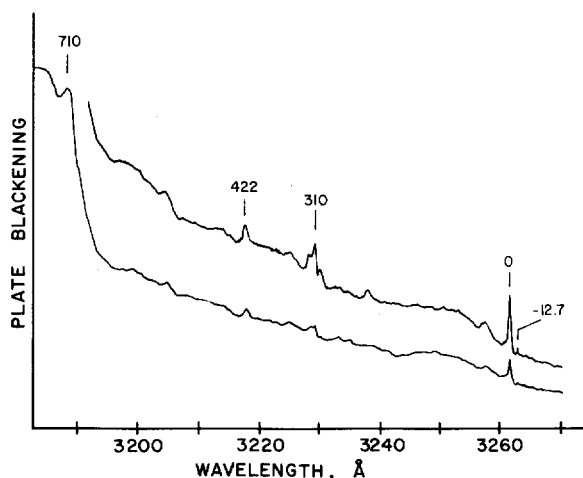


FIG. 14. Absorption spectrum at 4.2°K of 0.5% d_3 -*sym*-triazine in *sym*-trioxane mixed crystals 6 and 2.8 cm in length. Both of these samples were oriented such that the angle between the threefold crystal axis and the direction of light propagation was $\sim 85^\circ$. The distance in cm^{-1} from the origin (Region II, $30\,650.3 \pm 0.2 \text{ cm}^{-1}$) is marked above the major absorption features. The weak line $12.7 \pm 0.2 \text{ cm}^{-1}$ red of the origin is probably due to a $C_3D_2N_3$ pair. In this regard, compare with Fig. 13.

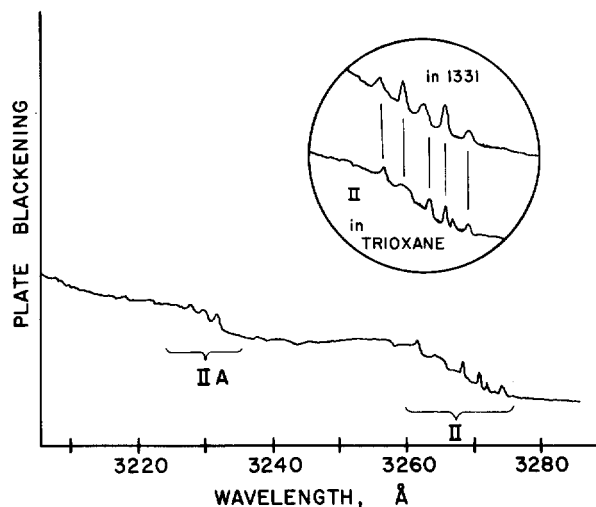


FIG. 15. Absorption spectrum at 4.2°K of 2% 1331-*sym*-triazine in a 1.5 cm *sym*-trioxane mixed crystal. The insert compares the Region II absorption in this trioxane host with that of a pure 0.5 mm 1331-*sym*-triazine crystal. For the 1331 in trioxane experiment, the three-fold crystal axis made an angle of $\sim 45^\circ$ with the direction of light propagation. This spectrum is discussed in the text (Sec. III.C).

(b) In all cases for which an orientational effect has been observed in organic molecular crystals it has been accompanied by a similar splitting of vibrational degeneracies (site group splitting).¹³ However, no such splitting has been observed in any crystal absorption of h_3 or d_3 species. In this connection it should be remembered that while *sym*-triazine is known to undergo a phase transition at $T \leq -60^\circ\text{C}$,¹⁰ trioxane is known to retain its threefold crystal axis at least down to -170°C .⁷ It is therefore expected that spectra of h_3 -*sym*-triazine in trioxane are more representative of a true threefold symmetric environment. Similarity of spectra in the two crystals is a good indication that no "site splitting" has occurred.

(c) Absorption features in Region II for h_3 and d_3 isotopic species do not split; nonetheless, as stated earlier, this transition is known to involve a doubly degenerate excited state. A crystal field asymmetry (i.e., site of lower than C_3 symmetry) of substantial size will split this degeneracy. Furthermore, since this site splitting $\Delta\nu_D$ would exist only in excited states, the totality of the effect would be evidenced directly in the optical transition. Since orientational effects in h_2d_1 and h_1d_2 isotopes are present in both ground and excited states, the magnitude of the resultant orientational splitting $\Delta\nu_{OE}$ in optical transitions will be substantially reduced. It is therefore quite reasonable to assume that $\Delta\nu_{OE} < \Delta\nu_D$. Figures 6-8 and 13 among others show $\Delta\nu_D$ much less than 2 cm^{-1} ; it is quite implausible that $\Delta\nu_{OE}$ could be as high as 25 cm^{-1} .

(d) Nearly complete superimposability of 1331 splitting patterns of Region I and Region II argues

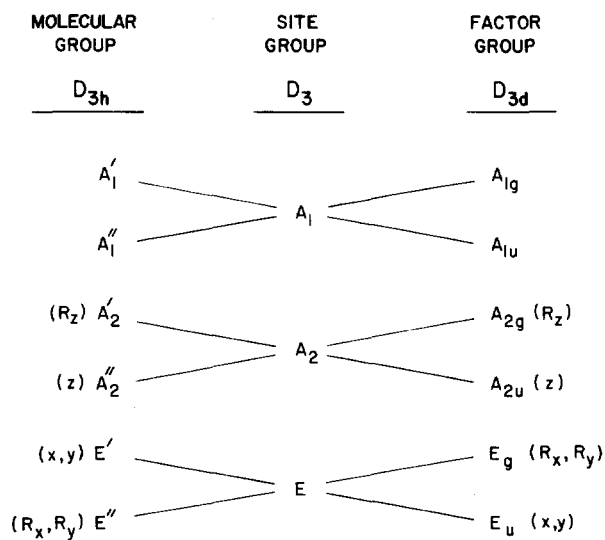


Fig. 16. Correlation diagram for the pertinent groups for *sym*-triazine in an $R\bar{3}c$ crystal.

against this splitting being controlled by orientational effects, which are essentially differences in gas-to-crystal shifts Δ . On the other hand, isotope effects seem to be constant for both singlets and triplets.¹³ Pyrazine is a good example of this observation¹⁴; for both singlet and triplet transitions $(E_{d_4} - E_{d_0}) = 155 \text{ cm}^{-1}$, while $\Delta_T = -556.2 \text{ cm}^{-1}$ and $\Delta_S = -951.5 \text{ cm}^{-1}$. Zeeman effect results¹ clearly indicate that Region I is a triplet state, while Region II is just as clearly an orbitally degenerate singlet state.

For these reasons we will proceed to assign spectra of *sym*-triazine on the basis that splitting of h_2d_1 and h_1d_2 isotopic species in Region II and Region I is a consequence of the zero point effect (3); that is, both absorption features involve transitions to *orbitally degenerate excited states*.

B. Assignment of Region I and Region II

Region I: Zeeman results on this transition indicate that the excited state is a triplet. The zero point effect splitting of C_{2v} isotopic species indicates that the state is an orbitally degenerate ${}^3E'(\pi\pi^*)$ or ${}^3E''(n\pi^*)$ state. Since ${}^1E'$ is believed to be some $2 \times 10^4 \text{ cm}^{-1}$ higher in energy than ${}^1E''$,¹⁵ it is *assumed* that such a low lying 3E state would be ${}^3E''(n\pi^*)$. Both sharp and broad emission from *sym*-triazine isotopic mixed crystals commencing at about 225 cm^{-1} red of Region I have been observed. This relatively intense emission must be assigned as either originating from a lower lying triplet state of *sym*-triazine or an impurity.⁴ Furthermore, the sharp initial Region I feature is virtually identical in all respects (i.e., isotope effect—see Secs. IV.A, IV.C, and IV.G; vibronic structure and phonon additions—see Figs. 3 and 5; apparent exciton effects—see Sec. IV.H) to the sharp initial

feature of Region II. This nearly exact similarity between Region I and Region II strongly argues against any assignment that gives Region I and Region II different character. *It is therefore believed that Region I is not a false vibronic origin and absorption in Region I is assigned to the ${}^3E''(n\pi^*) \leftarrow {}^1A_1'$ transition origin.*

Region II: The excited state terminus of this transition is an orbitally degenerate singlet state and since it is also a forbidden band, it is assigned as the ${}^1E''(n\pi^*) \leftarrow {}^1A_1'$ origin.

C. Nature of the Zero Point Effect

It is well known that, as a result of vibronic coupling, all electronic orbital degeneracies in polyatomic molecules are in principle converted into vibronic degeneracies.¹⁶ The $E''(n\pi^*)$ states assigned in Sec. IV.B. for h_3 - and d_3 -*sym*-triazine should present excellent examples of such vibronic coupling effects. An isotopic substitution which changes vibrational (nuclear) symmetry to C_{2v} will remove the original molecular *vibronic* degeneracy. The larger this vibronic coupling is for a particular vibronic state, the larger will be the splitting of that state upon asymmetric isotopic substitution.

If the above were the only source of splitting for C_{2v} isotopic species of *sym*-triazine, such observed splitting would constitute an exceptionally clear measure of the strength of vibronic coupling in a polyatomic molecule. It is, unfortunately, not the only source of such splitting; to *dynamic vibronic effects* must be added a set of *static* perturbations which, although perhaps small, cannot be neglected. The first of these static effects is a consequence of the fact that even at the equilibrium, "clamped nuclei" configuration, molecular symmetry is now C_{2v} for isotopically substituted molecules. However, contributions to the splitting from this effect are most likely vanishingly small. The main (static) effect arises with deviations from threefold symmetry in clamped nuclear configurations other than that at equilibrium. Since a change in effective mass of even a harmonic vibration is also reflected in a change of amplitude, distortion of the molecule from threefold symmetry becomes more pronounced as distance from equilibrium increases. The effect is obviously present in all vibrations, regardless of symmetry, and results in the splitting of degenerate electronic states in the asymmetric field of molecular vibrations.

The zero point effect thus comprises two parts: a static effect wherein electronic motion is dependent only upon instantaneous nuclear positions and a dynamic effect wherein linear and quadratic vibronic coupling terms exist which invalidate the normal (Born-Oppenheimer) separability of nuclear and electronic motions. Both types of effects will be quite a bit more sensitive to isotopic substitution within

the molecular ring than to substitution at hydrogen positions.

D. Zeeman and Stark Effects¹⁷

Zeeman and Stark effect experiments on Region II of *h₃-sym*-triazine¹ are consistent with 1331-*sym*-triazine Region II spectra obtained in the present investigation. The ¹E'' excited state assignment is thus confirmed by these results. It should be noted that a Stark effect experiment in Region II on a 1331 sample can *potentially* distinguish between site and zero point effect causes. If all lines are observed to split in a Stark field, no information is obtained; this result would be expected if either orientational or zero point effects produced observed splittings of C_{2v} isotopes. However, if only *h₃*- and *d₃-sym*-triazine lines were to split and not those of the C_{2v} species, then this would positively identify the zero point effect (that is, the orbital degeneracy has been removed in the molecule).

Results of Hochstrasser, Lin, and Zewail^{1a} on the Zeeman effect in Region I indicate that the τ_z(a₂' in D_{3h}) spin component is predominantly active in coupling this triplet state to the singlet manifold. Their polarization results at zero magnetic field give at least 85% of the total transition intensity as out of plane (z axis).¹⁸ This previous study concluded that Region I absorption must be to the ³A₁'(nπ*) excited electronic triplet state. It was argued that only for this state is it possible to mix in ¹A₂'(nπ*) or z character via a τ_z spin component if only direct matrix elements of the form ⟨¹A₂' | ℳ_{so} | ³A₁'(τ_z)⟩ are considered. Such a conclusion is rather surprising for two reasons: ³A₁'(nπ*) is not predicted to lie lowest¹⁹ and an nπ*-to-nπ*-state spin-orbit coupling route was found to predominate when an nπ*-to-ππ* route, ⟨¹E' | ℳ_{so} | ³A₁'(τ_x, τ_y)⟩, was also available.²⁰

Our experiments show, however, that absorption in Region I is due to the transition ³E''(nπ*)←¹A₁'. We are then immediately confronted with the problem of explaining the Zeeman results in the light of this assignment. Unfortunately, the present level of understanding of orbitally degenerate triplet states is quite inadequate.²¹ In fact, if our assignment is correct, *sym*-triazine is the first nonlinear, polyatomic molecule for which Zeeman results in an orbitally degenerate triplet state are known. Outlined below is *one possible explanation* of observed Zeeman patterns compatible with the ³E''(nπ*)←¹A₁' assignment of Region I. It is to be emphasized only that the previous explanation of these findings is not unique.

In an isolated molecule, assuming D_{3h} symmetry and no complications from vibrations, the only spin-orbit coupling route which mixes allowed character into the ³E''←¹A₁' transition can be expressed by the matrix element ⟨¹E' | ℳ_{so} | ³E''(τ_x, τ_y)⟩. Such a spin-orbit coupling route would be completely at variance with reported z polarization of Region I absorption, however.²² Since, for reasons previously

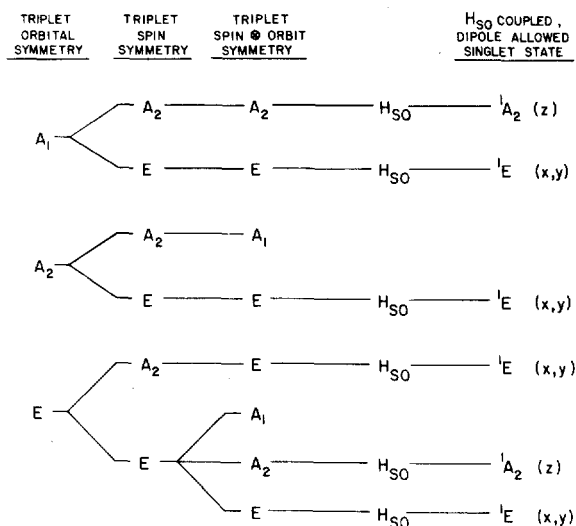


FIG. 17. Spin-orbit coupling routes for *sym*-triazine in a D₃ site. The last column indicates the singlet state which brings dipole allowed (E1) character into the triplet state 0-0 transition. Polarization of this transition is indicated in parentheses after the state.

stated, Region I has been assigned to the 0-0 transition of ³E''←¹A₁', otherwise available spin-orbit-vibronic routes cannot be invoked to eliminate this discrepancy.

The situation is different, however, in the crystal. In both *sym*-trioxane and *sym*-triazine crystals, site symmetry is reduced to D₃. (A correlation diagram for the various relevant symmetry groups can be found in Fig. 16.) Intensity of the ¹E''←¹A₁' 0-0 transition is essentially unaffected by the two different crystal fields. Therefore, it is the crystal site, not resonance or factor group interactions, that is responsible for bringing intensity into the (D_{3h}) forbidden origin. The substantial perturbation which crystal field interactions appear to have on out-of-plane vibrations may be another significant manifestation of this same effect (see Sec. IV.F and Ref. 2).

Figure 17 shows symmetry allowed spin-orbit coupling routes for site perturbed (D₃) *sym*-triazine. The ³E''(nπ*) molecular state has, under this perturbation, become ³E. Two specific features of this symmetry reduction are of particular concern to this line of reasoning. First, ³E''(nπ*) and ³E'(ππ*) states are mixed by the D₃ crystal site interactions. That these interactions are indeed substantial is evidenced by the large gas-to-crystal shift (Δ~ -850 cm⁻¹) for ¹E''(nπ*)←¹A₁'. Second, in addition to coupling to the ¹E'(ππ*) state which was allowed for a D_{3h} free molecule, crystal site interactions have made available other routes. One such route is characterized by the matrix element ⟨¹A₂(z) | ℳ_{so} | ³E(τ_x, τ_y)⟩. This route will now bring z-polarized intensity into the zero field levels. Assume for the moment that such a mechanism explains the zero magnetic field polarization results.¹⁸

TABLE II. Gas-to-crystal shift data Δ for ${}^1E''$ of *sym*-triazine in cm^{-1} . The gas phase values are 30 870 and 30 989 cm^{-1} for h_3 - and d_3 -*sym*-triazine, respectively.^a

Guest	Host		
	<i>d</i> ₃ - <i>sym</i> - Triazine (cm^{-1})	1331- <i>sym</i> - Triazine (cm^{-1})	<i>h</i> ₃ - <i>sym</i> - Triazine (cm^{-1})
<i>h</i> ₃ - <i>sym</i> -Triazine	-846	-851	-856
<i>d</i> ₃ - <i>sym</i> -Triazine	-846	-850	-856

^a Reference 2.

At values of external magnetic field such that $\mathcal{H}_z < \mathcal{H}_{c0}$, a field directed parallel to the crystal *c* axis will effectively not mix the A_2 spin-orbit (allowed) state with any of the others. The resulting optically observed Zeeman pattern will be a strong center line with weak wing lines. The wing intensity could arise from other spin-orbit mechanisms, such as $\langle {}^1E' | \mathcal{H}_{c0} | {}^3E''(\tau_x, \tau_y) \rangle$,²² from crystal field effects which lower site symmetry to perhaps C_s , and magnetic field state mixing. The pattern for external magnetic field perpendicular to the crystal *c* axis (in the molecular plane) will be a pair of strong wing lines and weak center one. This is exactly what is observed with unpolarized light at 30 kG.¹ However, when $\mathcal{H}_z \gg \mathcal{H}_{c0}$ Zeeman splitting patterns will change and will no longer be in agreement with observed results in as much as the spin-orbit coupling mechanism invoked here involves in-plane (τ_x, τ_y) spin components.

The above arguments are valid only if the A_2 multiplet state is split away from the A_1 state by roughly 5–10 cm^{-1} at zero field. Furthermore, the E state which derives from the (τ_x, τ_y) spin states must be no more than $\sim 0.1 \text{ cm}^{-1}$ from A_2 . Such a zero field splitting pattern may be caused by diagonal and off-diagonal spin-orbit coupling within the triplet manifold. Emission results⁴ and pronounced broadening of the absorption blue of Region I indicate that the ${}^3A_1'(\pi\pi^*)$ state may be less than 250 cm^{-1} from the ${}^3E''$ origin. Strong spin-orbit coupling (~ 30 –50 cm^{-1}) could take place between $A_2'(E'' \times e'')n\pi^*$ and $A_2'(A_1' \times a_2')\pi\pi^*$ sublevels of these two electronic states. The near degeneracy of the A_2 and E levels at zero field as measured by the published Zeeman results is not necessarily related, therefore, to the value of D , the noncubic (spin-spin) splitting parameter. Reported presence of a linear Stark Effect¹⁷ is easy to explain in this scheme if the most intense "allowed" spin-orbit substate is the A_2 multiplet component, which is virtually degenerate with the E component.

At present levels of understanding of spin-orbit coupling in degenerate states and Stark and Zeeman

effects on such states, it appears necessary to invoke considerable strength of spin-orbit coupling to explain field dependent experiments. Such strength may in fact be present in molecules of this type.²³ All of the foregoing discussion neglects linear and quadratic vibronic coupling which could be critically important for this degenerate state. Certainly there is much to be learned by a careful study of the interplay between the various and as yet poorly understood, phenomena possible for a 3E state. We are in the initial stages of such a study at present.

E. Gas-to-Crystal Shift

Data presented in Table II indicate that gas-to-crystal shifts for *sym*-triazines in isotopic mixed crystals of *sym*-triazine is independent of isotopic composition of guest molecules, but shows a uniform dependence upon isotopic composition of the host. In fact, in 1331 absorption studies, absorption line-width has increased such that it represents a distribution of sites from a local environment of purely h_3 nearest neighbors to purely d_3 nearest neighbors. Figure 12 illustrates this point. Line broadening is also present in the 1331 sample for the ${}^3E'' \leftarrow {}^1A_1'$ transition; its magnitude is apparently independent of whether the final state is a singlet or a triplet.

The ${}^1B_{3u}$ origin of pyrazine in *sym*-triazine mixed crystals has also been observed; it appears at 29 917.0 (± 0.5) cm^{-1} in *h*₃-*sym*-triazine and 29 925.4 (± 0.5) cm^{-1} in a *d*₃-*sym*-triazine host crystal. The energy of this transition has increased 8.4 cm^{-1} in the deuterated host, almost exactly paralleling observed changes in Δ for *sym*-triazine guest molecules in these hosts.

Similar dependences of guest molecule transition energy upon isotopic composition of host crystals have been noted by several other workers.²⁴ In particular, benzene has been studied quite carefully in this regard. *sym*-Triazine is a much more straightforward case since complications of factor group splitting and quasiresonance interactions are apparently negligible. Observations on *sym*-triazine bear a resemblance (perhaps superficial) to site interactions reported for pyrazine.²⁵ It is quite reasonable that the explanation of a deuterium isotope effect on Δ for pyrazine is similar to that in *sym*-triazine. The 10 cm^{-1} difference between the gas-to-crystal shift for guest molecules in *h*₃-*sym*-triazine (Δ_H) and the gas-to-crystal shift for guest molecules in *d*₃-*sym*-triazine (Δ_D) is thus ascribable to a change in lattice zero point energy and its coupling to guest molecules. Work is currently under way in our laboratory on this problem and its concomitant implications for lattice-molecule coupling interaction strengths.

F. Region III

Absorption spectra of a 0.5 mm crystal of 1331-*sym*-triazine, presented in Fig. 10, show that Region III

absorption does not appear to split for C_{2v} isotopic species. At first sight this would appear to be evidence that Region III is the origin of another (nondegenerate) electronic state. Severe difficulties arise, however, with this assignment. The absorption has been reported to be "mostly in-plane polarized"; less polarized, however, than the 0-0 band, Region II.^{26a} There are no nondegenerate states ($n\pi^*$ or $\pi\pi^*$) of *sym*-triazine which possess in-plane, crystal induced, $E1$ (electric dipole) intensity in their 0-0 transitions. Conceivably then, this is a false origin of another state, or a particularly strong triplet transition. However, the energy gap between Regions II and IIA is identical to within experimental uncertainty ($\sim \pm 1 \text{ cm}^{-1}$), to that between Region III and a similar feature, Region IIIA (see Fig. 3). The former separation was assigned by Fischer and Small² to the excited state out-of-plane (parallel) $\nu_4(a_2'')$, 737 cm^{-1} in the ground state).^{26b} It is thus possible to assign Region III as a transition to a vibration of the ${}^1E''$ excited electronic state. The most likely choice for this vibronic origin would be the out-of-plane mode $\nu_{16}(e'')$, 340 cm^{-1} in the ground state). Such an assignment is compatible with known in-plane polarization and appearance of an a_2'' combination band at Region IIIA.²⁷ Due to vibronic coupling, three absorptions may overlap in this region corresponding to $E'' \times e'' = E' + A_2' + A_1'$ vibronic states. The strong, reasonably sharp feature commencing Region III may correspond to one of the nondegenerate vibronic states; thereby explaining lack of splitting of this peak for C_{2v} species.

When comparing spectra of h_3 -*sym*-triazine in trioxane with those of h_3 -*sym*-triazine crystals, it is clear that the concomitant change in crystal field has had a substantial effect on those vibrations which have been assigned² as out-of-plane modes (ν_4 , ν_8 , ν_{10} , and ν_{16}), whereas little change is seen for in-plane vibrations. Crystal field effects are, in particular, quite severe for Region III absorption. The recent paper by Jesson, Krote, and Ramsey²⁸ concerning possible "quasi-planarity" in the first excited singlet state of pyridine suggests an interesting parallel for *sym*-triazine.²⁹ The vibrational mode which these authors suggest is responsible for anomalous absorption in pyridine is $\nu_{166}(b_2)$, 403 cm^{-1} in the ground state). This vibration derives from ν_{16} of benzene (e_{2u} , 405 cm^{-1} in the ground state), as does the ν_{16} of *sym*-triazine. It appears quite possible, through Region III identification as the ν_{16} vibronic origin, that *sym*-triazine is likewise highly anharmonic in this state. There are strong parallels between vibronic structure in ${}^3E'' \leftarrow {}^1A_1'$ and ${}^1E'' \leftarrow {}^1A_1'$ (Regions I and II, respectively). However, vibrational structure in these transitions is exceedingly complex and at the present time there are insufficient data to warrant any more than this quite tentative assignment of observed features.

G. ${}^{13}\text{C}/{}^{15}\text{N}$ Splitting in the ${}^3E''$ and ${}^1E''$ States

Figure 6(a) shows an expanded trace of fine structure around the ${}^3E'' \leftarrow {}^1A_1'$ origin in a 3.3 cm *sym*-triazine crystal and Table I contains a listing of these data. Similar structure is found around the ${}^1E''(n\pi^*) \leftarrow {}^1A_1'$ absorption origin [Fig. 6(b) and Table I] in a 1.5 mm thick crystal. For this molecule, isotopic natural abundances yield 3.2% ${}^{13}\text{C}{}^{14}\text{N}_3\text{H}_3$ and 1.1% ${}^{15}\text{N}{}^{13}\text{C}_2\text{N}_2\text{H}_3$. In absence of spectra of selectively isotopically enriched samples, of course, it can only be assumed that the observed structure is due to the above isotopes of *sym*-triazine. The third peak to the red of ${}^{12}\text{C}_3{}^{14}\text{N}_3\text{H}_3$ absorption is good indication of a sizeable (of the order of 10 cm^{-1}) zero point effect for one or both of these C_{2v} isotopes. Since only three and not four lines are observed, assignment of features to specific isotopes is not possible. Intensity considerations alone can be misleading due to poor resolution, accidental coincidences of isotopic lines, and C_{2v} selection rules for $E1$ transition moment character. Moreover, ${}^{13}\text{C}/{}^{15}\text{N}$ isotopic lines can selectively gain relative intensity from interactions with narrow but finite exciton bands. The situation can be further complicated by possible accidental coincidence with host-guest perturbed features in heavily doped (greater than 2%) mixed crystals [see Ref. 25 and Fig. 6(b)].

Oriental effects of magnitude greater than 1.0 cm^{-1} are not expected for ${}^{13}\text{C}$ - or ${}^{15}\text{N}$ -substituted aromatic rings since such small relative changes in molecular vibrations are involved and ring atoms are less directly involved in intermolecular interactions than hydrogen atoms. In fact, to our knowledge, no orientational effects have yet been reported for ring-substituted isotopic species. However, as was pointed out in Sec. IV.C, a substantial zero point effect is expected to accompany isotopic substitution on the ring. A 10 cm^{-1} splitting for ${}^{15}\text{N}$ and ${}^{13}\text{C}$ C_{2v} isotopes is therefore an excellent indication that it is the zero point effect, and not orientational effects, which is responsible for observed splitting of reduced symmetry isotopes of *sym*-triazine.

Future plans for this work include synthesis of highly enriched ${}^{13}\text{C}$ - and ${}^{15}\text{N}$ -*sym*-triazine samples for spectroscopic investigation.

H. Resonance Interactions, Gas-to-Crystal Shifts, and Intermolecular Interactions

There are four observations made in this investigation that bear on types of interactions that take place in a *sym*-triazine crystal (see Tables I and II):

1. Δ is large ($\sim -850 \text{ cm}^{-1}$) for the ${}^1E''(n\pi^*) \leftarrow {}^1A_1'$ transition.
2. Δ appears to be a function of isotopic composition of host crystal system only, $(\Delta_D - \Delta_H) \approx 10 \text{ cm}^{-1}$ and $(\Delta_D - \Delta_{1331}) \approx (\Delta_{1331} - \Delta_H) \approx 5 \text{ cm}^{-1}$.

3. Pure crystals, dilute isotopic mixed crystals, and 1331 samples yield constant "guest" energies to within the linewidth of a 1331 transition.

4. $^{13}\text{C}^{12}\text{C}_2\text{N}_3\text{H}_3$ and $^{15}\text{NC}_3^{14}\text{N}_2\text{H}_3$ lines can be identified to higher and lower energies about both the ${}^3E''(n\pi^*)\leftarrow{}^1A_1'$ and ${}^1E''(n\pi^*)\leftarrow{}^1A_1'$ origins in pure h_3 - and d_3 -*sym*-triazine crystals.

One concludes from these facts that dispersion forces (van der Waals interactions) responsible for Δ are large and that exchange interactions, both translationally equivalent and interchange equivalent, are probably not greater than 1 cm^{-1} .³⁰ In other words, the ${}^3E''$ and ${}^1E''$ states of *sym*-triazine have less than 1 cm^{-1} exciton bandwidths. Moreover, it appears that molecular electronic levels couple to lattice modes in such a way as to cause a change in Δ dependent on the isotopic composition of host crystal only. This energy difference may well be associated with a lattice zero point motion; either this motion or its coupling to guest molecules must change upon guest excitation.

I. Linewidths and Intensities in Pure and Mixed Crystals

In crystals of high optical quality, linewidths for both Region I and Region II are comparable. Region I (${}^3E''\leftarrow{}^1A_1'$) linewidths were generally less than 1.0 cm^{-1} in all crystals of all orientations. However, Region II (${}^1E''\leftarrow{}^1A_1'$) yielded linewidths that varied between 1 and 4 cm^{-1} with no apparent correlation between linewidth and purity, crystal quality, or strains. It is believed possible that this observed dramatic linewidth variability is primarily due to polarization effects. Sharpest spectra were seen in unpolarized light for a crystal most likely oriented with the *c* axis parallel to the direction of light propagation. Clearly this phenomenon deserves more extensive study.

The observed intensity pattern for Regions I and II in 1331-*sym*-triazine is roughly 1:1.5:1:1.5:1 (for an unresolved center line). Under C_{2v} distortion $E''\rightarrow A_2+B_2(z)$ and the A_2 state is E_1 forbidden. One naively expects only one line to be strong in the C_{2v} spectrum. The fact that both components are observed to have nearly equal intensity is, therefore, highly interesting. Apparently crystal field (site) or Jahn-Teller perturbations (the "dynamic" part of the zero point effect) have had a rather substantial effect on optical intensities.

V. CONCLUSION

A number of positive conclusions concerning *sym*-triazine and its mixed and pure crystals can be reached based on work presented in this paper. These main points are listed below.

1. The 3455 Å system of *sym*-triazine (Region I)

arises from the ${}^3E''(n\pi^*)\leftarrow{}^1A_1'$ transition. Strongest evidence for this assignment comes from D, H, ^{15}N , ^{13}C isotopic substituted (C_{2v}) *sym*-triazines.

2. Zeeman and Stark effect data previously published seem consistent with large diagonal [${}^3E''(n\pi^*)\leftarrow{}^3E''(n\pi^*)$] and off-diagonal [${}^3E''(n\pi^*)\leftarrow{}^3A_1'(\pi\pi^*)$] spin-orbit coupling interactions.

3. Based on Conclusions 1 and 2, "optically observed" zero field splitting need not give an accurate assessment of the noncubic zero field splitting term D . D may contain substantial contributions from both spin-orbit and spin-spin interactions.

4. This work confirms the previous assignment of the absorption at 3330 Å as due to the ${}^1E''\leftarrow{}^1A_1'$ transition (Region II). Therefore, all observed absorption features can be accounted for based on only two $n\rightarrow\pi^*$ transitions, ${}^3E''(n\pi^*)\leftarrow{}^1A_1'$ (Region I) and ${}^1E''(n\pi^*)\leftarrow{}^1A_1'$ (Region II).

5. There is apparently a sizeable molecule-lattice mode zero point coupling which could be responsible for $(\Delta_H-\Delta_D)\sim 10\text{ cm}^{-1}$. It is believed that deuterium substitution of the host causes a change in zero point energy or motion of the lattice which in turn affects the transition energy of both identified electronic transitions.

6. Both translationally equivalent and translationally inequivalent exciton interactions are small ($\leq 1.0\text{ cm}^{-1}$) in *sym*-triazine crystals. The most striking evidence for this is found in spectra of 1331-*sym*-triazine crystals as compared to pure and isotopic dilute mixed crystal spectra of h_3 - and d_3 -*sym*-triazine (Table I). Observation of $^{13}\text{CC}_2\text{N}_3\text{H}_3$ and $^{15}\text{NC}_3\text{N}_2\text{H}_3$ ${}^3E''(n\pi^*)\leftarrow{}^1A_1'$ and ${}^1E''(n\pi^*)\leftarrow{}^1A_1'$ transitions is also an indication of very small exciton bands.

7. Unlike exciton interactions, "crystal field" (site) dispersion or van der Waals terms are substantial ($\Delta\approx -850\text{ cm}^{-1}$ for ${}^1E''\leftarrow{}^1A_1'$).

8. Further evidence for large site effects can be found by comparing chemical mixed crystals (trioxane) with isotopic mixed or pure crystals. Out-of-plane (large amplitude) vibrations are most affected and Region III, tentatively assigned as $(0-0+\nu_{16}')$ of ${}^1E''\leftarrow{}^1A_1'$, typifies this large crystal site perturbation.

9. The only vibrational assignment made in this work is for Region III and even this must be considered only somewhat more reasonable, at the present time, than other possibilities. Region III has been assigned as ${}^1E''(n\pi^*)\leftarrow{}^1A_1'(0-0+\nu_{16}')$.

Note added in proof: Since submission of this paper, high field Zeeman and Stark effect data have been obtained [E. R. Bernstein and R. E. Smalley, *J. Chem. Phys.* (to be published)]. Spectra taken at 100 kG for D_{3h} and C_{2v} isotopes give no indication that either Region I or Region II absorptions involve orbitally degenerate states. Region I is clearly triplet state and Region II is a singlet state. In the process of verifying

Stark data of Ref. 17, it has been determined that both C_{2v} and D_{3h} isotopes show identical Stark splittings in a *sym*-triazine host crystal. Although tentative assignment of these regions as ${}^3E'' \leftarrow {}^1A_1'$ and ${}^1E_1'' \leftarrow {}^1A_1'$ is still favored, the situation is clearly more complex than previously assumed. Absence of a proof that the Region II absorption is to a degenerate state allows for other interpretations of these spectra not brought out in this paper. Experiments are currently underway to resolve apparent conflicts between Stark, Zeeman, Stark-Zeeman, and absorption data on the various isotopes.

ACKNOWLEDGMENTS

We wish to thank Professor G. J. Small (Iowa State University) for discussions concerning *sym*-triazine and for communication of his data prior to their publication. We have had further helpful discussions with Professor D. S. McClure and Dr. T. D. Brownrigg (Princeton University).

* This work was supported in part by the Army Research Office—Durham and the Office of Naval Research.

¹ (a) R. M. Hochstrasser, T. S. Lin, and A. H. Zewail, *J. Chem. Phys.* **56**, 637 (1972); (b) R. M. Hochstrasser and A. H. Zewail, *J. Chem. Phys.* **55**, 5291 (1971); (c) R. M. Hochstrasser and A. H. Zewail, *Chem. Phys. Lett.* **11**, 157 (1971); (d) R. M. Hochstrasser and T. S. Lin, *Symp. Faraday Soc.* **3**, 100 (1969).

² (a) G. Fischer and G. J. Small, *J. Chem. Phys.* **56**, 5934 (1972). (b) G. Fischer, *J. Chem. Phys.* **57**, 2646 (1972).

³ K. K. Innes, J. P. Byrne, and I. G. Ross, *J. Mol. Spectrosc.* **22**, 125 (1967).

⁴ E. R. Bernstein and R. E. Smalley (unpublished results).

⁵ L. E. Hinkel and R. T. Dunn, *J. Chem. Soc. (London)* **1930**, 1834.

⁶ C. Grundman and A. Kreutzberger, *J. Am. Chem. Soc.* **76**, 632, 5646 (1954).

⁷ V. Busetti, A. Del Pra, and M. Mammi, *Acta. Cryst.* **B25**, 1191 (1969).

⁸ V. Jaacks and W. Kern, *Macromol. Chem.* **52**, 37 (1962); *J. Polymer Sci.* **48**, 399 (1960); W. K. Busfield and D. Merigold, *J. Chem. Soc. (London)* (A) **1969**, 2975.

⁹ F. Wunder and H. Fernholz, German Patent No. 1,280,884 (1968) (*Chem. Abstr.* **70**, P20478K).

¹⁰ P. Coppens and T. M. Sabine, *Mol. Cryst.* **3**, 507 (1968).

¹¹ R. M. Hochstrasser and C. J. Marzocco, *J. Chem. Phys.* **49**, 971 (1968).

¹² The commerial syntheses are almost certainly using the formamide route; C. L. Sloan and W. A. Barber, U.S. Patent 3,133,062 (*Chem. Abstr.* **61**, 4379C).

¹³ (a) E. R. Bernstein, *J. Chem. Phys.* **50**, 4842 (1969); (b) E. R. Bernstein, S. D. Colson, D. S. Tinti, and G. W. Robinson, *J. Chem. Phys.* **48**, 4632 (1968); (c) G. C. Nieman and D. S. Tinti, *J. Chem. Phys.* **46**, 1432 (1967).

¹⁴ D. S. McClure and E. Zalewski (unpublished results); and E. Zalewski, (thesis, University of Chicago 1968). See also Ref. 3.

¹⁵ J. S. Brinen, R. C. Hirt, and R. G. Schmitt, *Spectrochim. Acta.* **18**, 863 (1962).

¹⁶ H. C. Longuet-Higgins, *Adv. in Spectro.* **2**, 429 (1961).

¹⁷ The observation of a linear Stark splitting of Region I absorption by D. A. Wiersma (private communication) became known to us after this paper was completed. This Stark experiment result is completely in accord with the conclusions of this paper. D. A. Wiersma, *Chem. Phys. Lett.* **16**, 517 (1972).

¹⁸ It should be pointed out, however, that, in general, polarization experiments for *sym*-triazine at low temperature ($T \leq -60^\circ\text{C}$) are somewhat of a problem. Even though the -60°C phase transition has a negligibly small effect on electronic spectra, the crystal has gone from optically uniaxial to optically biaxial. Light in the crystal, especially for a plate cut parallel to the uniaxial (room temperature) optic axis, is always elliptic in nature. The 2 optic axes in the biaxial modification are probably greater than 10° apart (see Ref. 10).

¹⁹ J. S. Brinen and L. Goodman, *J. Chem. Phys.* **31**, 482 (1959).

²⁰ J. W. Sidman, *J. Mole. Spectro.* **2**, 333 (1958); M. A. El-Sayed, *J. Chem. Phys.* **38**, 2834 (1963); L. Goodman and V. Krishna, *Rev. Mod. Phys.* **35**, 541 (1963); E. Clementi and M. Kasha, *J. Mole. Spectro.* **2**, 297 (1958).

²¹ J. H. van der Waals and M. D. de Groot, *The Triplet State—Beirut Symposium*, 1967, edited by A. B. Zahlan (Cambridge U. P., London, England, 1967), p. 101ff.

²² The spin-orbit coupling between the ${}^3E''$ and ${}^1E'$ states is expected to be quite small due to cancellation of one-center terms. Some in-plane dipole intensity should be present in the ${}^3E''$ transition due to spin-orbit coupling with the ground state. [R. M. Hochstrasser (private communication) and *Chem. Phys. Letter.* **17**, 1 (1972)].

²³ H. M. McConnell, *J. Chem. Phys.* **34**, 13 (1961).

²⁴ (a) S. D. Colson, *J. Chem. Phys.* **48**, 3324 (1968), and S. D. Colson and T. L. Netzel (private communication) and *Chem. Phys. Lett.* **16**, 555 (1972); (b) D. M. Burland, G. Castro, and G. W. Robinson, *J. Chem. Phys.* **52**, 4100 (1970); (c) R. M. Hochstrasser and J. D. Whiteman, *J. Chem. Phys.* **56**, 5945 (1972).

²⁵ E. F. Zalewski and D. S. McClure, *Molecular Luminescence*, edited by E. C. Lim (Benjamin, New York, 1969), p. 739ff.

²⁶ (a) G. J. Small (private communication); (b) Ref. 2; note that there is an inconsistency in labeling of vibrations in Fig. 6 as compared with assignments appearing in Table III of this reference—Table III is correct. G. J. Small (private communication).

²⁷ It should be noted that the d_3 spectrum does not show a prominent feature in Region IIIA. However, Region IIIA in the d_3 spectrum is clearly not free of absorption and the apparent absence of the Region IIIA feature here may be due to broadening through enhanced vibronic interaction.

²⁸ J. P. Jesson, H. W. Kroto, and D. A. Ramsay, *J. Chem. Phys.* **56**, 6257 (1972).

²⁹ Pyrazine spectra may also be so interpreted, D. S. McClure (private communication).

³⁰ A. S. Davydov, *Theory of Molecular Excitons* (Plenum, New York, 1971); S. A. Rice and J. Jortner, *Physics and Chemistry of the Organic Solid State*, edited by D. Fox, M. M. Labes, and A. Weissberger, (Interscience, New York, 1967), Volume III, p. 199ff; E. R. Bernstein, S. D. Colson, R. Kopelman, and G. W. Robinson, *J. Chem. Phys.* **48**, 5596 (1968).